

Thermal Conductivity of Self-Assembling Symmetric Block Copolymer Thin Films of Polystyrene-Block-Poly(methyl methacrylate)

Matthew C. George

Moxtek,
Orem, UT 84057;
Sandia National Laboratories,
Albuquerque, NM 87185
e-mail: mgeorge@moxtek.com

Mark A. Rodriguez

Sandia National Laboratories,
Albuquerque, NM 87185

Michael S. Kent

Sandia National Laboratories,
Albuquerque, NM 87185

Geoff L. Brennecka

Metallurgical and Materials Engineering,
Colorado School of Mines,
Golden, CO 80401;
Sandia National Laboratories,
Albuquerque, NM 87185

Patrick E. Hopkins

Department of Mechanical and Aerospace Engineering,
University of Virginia,
Charlottesville, VA 22904
e-mail: phopkins@virginia.edu

The thermal conductivities of both disordered and self-assembled symmetric polystyrene-block-poly(methyl methacrylate) (PS-b-PMMA) copolymer films were measured using time-domain thermoreflectance (TDTR). The variation in out-of-plane thermal conductivity with changing block copolymer thickness is similar to that of PMMA polymer brushes and thick spun-cast films. The results suggest that the interfaces between the PS and PMMA, and reorganization of the PS and PMMA chains around these interfaces, do not significantly affect the thermal transport in these PS-b-PMMA films. However, for thin PS-b-PMMA films, the thermal boundary resistances at the sample interfaces limit the thermal transport. [DOI: 10.1115/1.4031701]

Keywords: thermal conductivity, heat transfer in block copolymer thin films, thermal boundary conductance, time-domain thermoreflectance, interfacial chain alignment

1 Introduction

The control of thermal transport properties using nanoscale materials is an increasingly important area of research in the fields of electronic devices and energy conversion technologies [1,2]. Recent

works exploring low-dimensional systems and multiphase nanocomposites with engineered phonon scattering properties have led to new regimes and extremes of heat conduction [3]. Many of these advances have relied on soft materials and polymeric-based systems that have, for example, set new lower limits for the thermal conductivity of fully dense solids [4], demonstrated orders of magnitude changes in thermal conduction based on alignment, rigidity, or draw ratio [5–8], and shown intricate tunability in vibrational heat transfer based on side chain and compositional perturbations [9–11]. Because of this immense promise in thermal engineering of polymers, recent research has focused on vibrational energy coupling across polymeric interfaces to engineer the thermal conductivity of molecular-based composites [12–17]. These works have relied on the coupling of energy across organic/inorganic interfaces or focused on C₆₀ or carbon nanotube/polymer-based composites [12–20], whereas experimental quantification of the influence of polymer/polymer planar interfaces on thermal transport is nonexistent, to the best of our knowledge.

While bulk polymers are generally regarded as good thermal insulators with typical thermal conductivities on the order of 0.1 W m⁻¹ K⁻¹, both experimental and computational works have demonstrated an increase in thermal conductivity (decrease in thermal resistance) upon straining due to increased polymer chain alignment and crystallization [6,8,21–23]. For example, ultradrawn polyethylene micro- and nanofibers have been shown to have a 120- to 300-fold increase in their thermal conductivity along the draw direction due to a large fraction of long needlelike crystals with chain orientations parallel to the draw direction [6,12,18–22], and in PMMA, up to a 50% increase in axial thermal conductivity has been observed in fibers for draw ratios of only 4 [24,25]. On the contrary, in studies of PMMA polymer brush samples, only modest increases of less than 10% in axial thermal conductivity were observed [26], and for ultrathin spun-cast PMMA films, the intrinsic thermal resistances were comparable to the thermal boundary resistances at the film/substrate interfaces, leading to a reduction in the effective thermal conductivity [26]. However, studies using spun-cast polyimide films demonstrated a reduction in out-of-plane thermal conductivity with a concomitant increase in the in-plane thermal conductivity by a factor of 4–8 [27].

As evident from these aforementioned studies, chain alignment and material boundary resistances can affect thermal transport in nanoscale confined polymers, polymer brushes, and self-assembled monolayers. However, there has been little research into the nanoscale thermal transport behavior of thin self-assembled block copolymer films, which can contain high densities of polymer/polymer interfaces and varying degrees of chain alignment and interfacial ordering. A more detailed understanding of the thermal conductivity of block copolymer films could help reveal the relative roles of polymer–polymer interfaces and chain alignment on the heat transfer mechanisms of polymeric-based nanosystems.

Motivated by the need for elucidation into how polymer–polymer interfaces and chain alignment affect thermal transport in organic systems, this work experimentally studies the thermal conductivity of a series of block copolymer films. Block copolymer materials have been steadily garnering increased attention due to their ability to form nanoscale periodic structures at time-scales of industrial relevance [28,29]. Symmetric PS-b-PMMA is a well-studied model diblock copolymer system that is thermodynamically and kinetically amenable to directed self-assembly into controlled lamellar phases, hence these materials represent good candidates for studying the role of polymer ordering and interfaces on thermal conductivity in organic systems. A symmetric PS-b-PMMA block copolymer was chosen that naturally forms a lamellar phase with periodicity (L_0) of about 27.5 nm [30]. A polar silicon thermal oxide substrate was chosen in order to drive the PMMA block toward the substrate at elevated temperatures, initiating directed self-assembly such that the lamellar periodicity, and any preferential chain alignment, would be normal to the substrate surface. This work utilizes TDTR to measure the thermal conductivity of PS-b-PMMA films with varying thicknesses

Contributed by the Heat Transfer Division of ASME for publication in the JOURNAL OF HEAT TRANSFER. Manuscript received March 5, 2015; final manuscript received August 13, 2015; published online October 21, 2015. Assoc. Editor: Alan McGaughey.

The United States Government retains, and by accepting the article for publication, the publisher acknowledges that the United States Government retains, a nonexclusive, paid-up, irrevocable, worldwide license to publish or reproduce the published form of this work, or allow others to do so, for United States government purposes.

in both random and ordered states in order to understand the impact of chain alignment, interfacial ordering, and the role of thermal boundary resistances on the thermal conductivity of PS-*b*-PMMA films. This work specifically aims to answer the question: What energy transport mechanism is more dominant in the heat transport within the block copolymer films—chain alignment and internal ordering (layer formation) or thermal boundary resistances?

2 Experimental Considerations

2.1 Sample Fabrication and Characterization. The PS-*b*-PMMA films were spun-cast from propylene glycol monomethyl ether acetate solutions to thickness values commensurate with the asymmetric wetting condition and the natural lamellar period of the block copolymer, as verified by ellipsometry prior to annealing. The spun-cast films were initially amorphous and were then cleaved with one set annealed in a vacuum oven (Yamamoto) below the order-disorder transition temperature, but well above the glass

transition temperature, in order to promote directed self-assembly into the asymmetric lamellar phase. The optimum temperature for assembly was determined by performing self-assembly of the block copolymer on neutral polymer brush layers (forming fingerprint patterns). The polar substrate and nonpolar vacuum ambient produced an asymmetric wetting condition for the assembled lamellar phase [31–34], schematically depicted in Fig. 1, along with X-ray reflectivity (XRR) data and modeling for various film thicknesses and annealing states, which shows excellent agreement with the experimental data for both the unannealed and annealed block copolymer states. The idealized PS-*b*-PMMA lamellar phase depicted in Fig. 1(a) has a thickness $t_n = (n + 1/2)L_0$, where n is the number of full lamellar periods L_0 , which was varied from 0 to 7. The surface roughness of spun-cast and annealed PS-*b*-PMMA films was typically about 5 Å and 2 Å, respectively, as measured by atomic force microscopy (AFM). As presented in Table 1, only films with thickness commensurate with t_n , the asymmetric lamellar assembly condition, were utilized in this study and no terracing or holes in the films were observed. The assembly of the annealed films into the

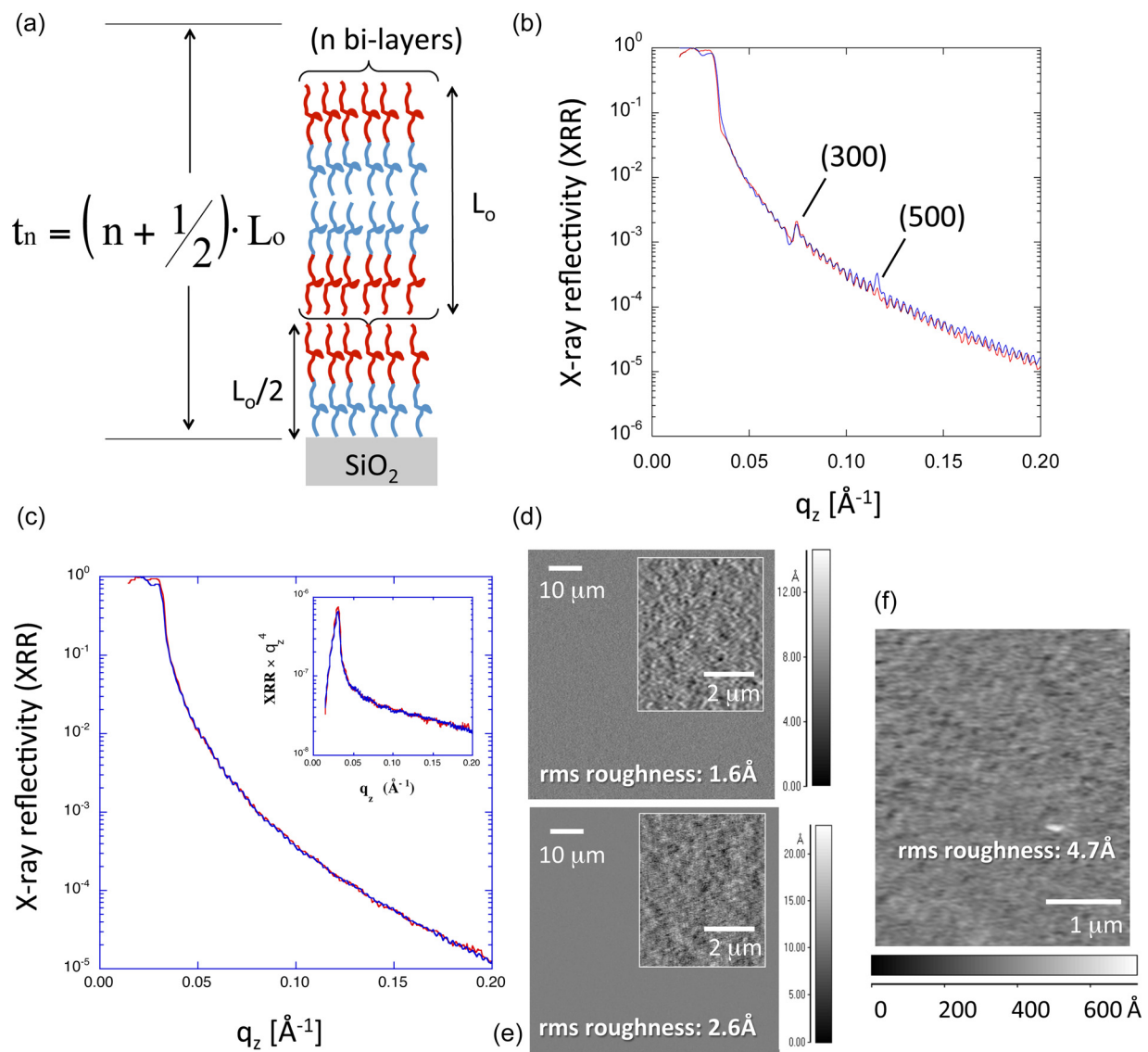


Fig. 1 (a) Block copolymer assembly schematic for the asymmetric wetting condition. (b) and (d) XRR data and modeling. (b) Thick annealed film commensurate with 6.5 lamellar periods (L_0) showing third- and fifth-order Bragg peaks, (c) thick unannealed film (plotted as $XRR \times q_z^4$ to display the weak high frequency oscillations in the data), (d) and (e) large area AFM deflection mode images (with inset topography images) depicting surface roughness of annealed films commensurate with 1.5 (d) and 6.5 (e) lamellar periods. (f) AFM topography image of spun-cast film before annealing. These AFM images confirm that the films did not dewet and remained conformal after annealing.

Table 1 Film thickness before annealing as measured by ellipsometry

Thickness (nm)	Expected # of lamellar periods ($n + 0.5$)	% deviation from t_n
201.7 ± 2.4	7.5	-3.9
183.3 ± 0.6	6.5	0.7
160.5 ± 0.1	5.5	4.2
129.0 ± 0.7	4.5	2.4
99.1 ± 1.2	3.5	1.1
71.4 ± 2.5	2.5	2.1
41.8 ± 0.2	1.5	-0.4
15.3 ± 0.05	0.5 (++)	9.2
14.7 ± 0.04	0.5 (+)	4.9
14.1 ± 0.06	0.5	0.4
13.1 ± 0.06	0.5 (-)	-6.6

stacked asymmetric lamellae was verified by XRR measurements and representative results are presented in Fig. 1. In the absence of block copolymer ordering, the electron density difference between silicon and the polymer leads to oscillations in the reflectivity (Kiessig fringes), which are indicative of the overall film thickness. When the block copolymer forms lamellae, the small difference in electron density between PS and PMMA is sufficient to produce Bragg peaks due to reflections from the PS and PMMA layers. XRR from annealed films with fewer than 2.5 lamellar periods does not show Bragg peaks, but XRR from thicker films shows diffraction peaks that increase in intensity with the number of lamellar periods n . XRR from unannealed films does not show Bragg peaks, regardless of film thickness. Figures 1(b) and 1(c) depict XRR results for a film of thickness commensurate with 6.5 lamellar periods after annealing and without annealing, respectively. In Fig. 1(b), the XRR measurement and modeling results show that only the odd order Bragg peaks are present, consistent with the choice of a symmetric PS-b-PMMA copolymer [35]. The (300) peak is clearly evident in the data. Atomic force microscopy analysis (Figs. 1(d)–1(f)) confirms the similar topology of each film regardless of annealing condition and demonstrates that the films do not dewet and remain conformal during after annealing.

2.2 TDTR. After XRR measurements, an aluminum metal transducer was evaporated on the surface of the films as a transducer for thermal conductivity studies using TDTR [36–38], which is a noncontact, pump-probe technique in which a modulated train of subpicosecond laser pulses is used to create a heating event (the pump) on the surface of a sample. This pump-heating event is then monitored with a series of time-delayed probe pulses. The probe pulses are detected at the modulation frequency of the pump train through a lock-in amplifier over about 4.0 ns of probe delay time to determine the change in aluminum reflectivity with time, which is related to the temperature change on the surface of the sample. This surface temperature data are then related to the out-of-plane thermal conductivity (κ) of the PS-b-PMMA films through a thermal model accounting for the radial symmetry of the heating event, pulse accumulation, and thermal diffusion mechanisms through the various layers of sample [37,39,40]. For determining the thermal conductivity of the PS-b-PMMA film, the model was fit to the data by iterating the thermal conductivity as a free parameter while assuming literature values for the heat capacities of the Al and SiO₂ films, the Si substrate [41], and PS and PMMA layers [42,43], as well as literature values for the Si and SiO₂ thermal conductivities [41,44], and an Al film thermal conductivity based on previous measurements of Al films deposited using the same evaporator (166 W m⁻¹ K⁻¹) [40]. Thicknesses of the Al films were approximately 83 ± 3 nm, as confirmed using picosecond acoustics [45,46]. An example of the TDTR data and the corresponding best fit model are shown in Fig. 2(b). The total thermal resistance determined using TDTR is a

combination of the resistances offered by the PS-b-PMMA film and the polymer–inorganic interfaces R_{12} and R_{23} , as depicted in Fig. 2(a) for an assembled PS-b-PMMA sample. Due to the low thermal conductivities of the PS-b-PMMA films, the measurements are insensitive to the Al/PS-b-PMMA and PS-b-PMMA/SiO₂ interfacial resistances, resulting in a high sensitivity to fitting of the thermal conductivity of the PS-b-PMMA film. However, as discussed in Sec. 3, for the thinnest samples, the resistances offered by the PS-b-PMMA films are on the order of the thermal boundary resistances at the film interfaces, and therefore the resistances of the Al/PS-b-PMMA and PS-b-PMMA/SiO₂ interfaces influence the measured effective thermal conductivities.

3 Results and Discussion

Figure 2(c) shows the experimentally measured thermal conductivity of both ordered (annealed) and disordered (amorphous) PS-b-PMMA copolymer films as a function of film thickness. The measurements are compared to previous reports of the thermal conductivity of thin PMMA homopolymer films and polymer brushes reported by Losego et al. [26], which showed a modest increase in out-of-plane κ for elongated, grafted PMMA polymer brushes when compared to the random coil chain configurations inherent in bulk PMMA. However, the amorphous and ordered PS-b-PMMA films measured in our current study exhibit thermal conductivities similar to the bulk homopolymer values (0.17 and 0.20 W m⁻¹ K⁻¹ for PS and PMMA, respectively) [47]. For the thinnest samples ($t_0 \approx 14$ nm $\approx L_c/2$), an effective thermal conductivity (κ_{eff}) is plotted, which includes thermal resistances at the interfaces between the PMMA block and thermal oxide and between the PS block and aluminum. This approach is used because the thermal resistance offered by the PS-b-PMMA film is on the same order as the resistances at the polymer–inorganic interfaces, and the TDTR measurement approach cannot differentiate between the three series resistances (Fig. 2(a)) for these very small PS-b-PMMA film thicknesses. These results are discussed in more detail below.

Losego et al. [26] observed a reduction in thermal conductivity for extremely thin spun-cast PMMA films, where the resistance offered by the PMMA film was on the order of the thermal boundary resistances at the film interfaces. Likewise, in the current study, the reduced out-of-plane κ_{eff} in the thinnest PS-b-PMMA samples, for both amorphous and annealed cases, is likely due to the incorporation of interfacial resistances at the Al/sample and sample/substrate boundaries (similar to the conclusions by Losego et al. [26]), rather than any polymer/polymer interface or chain alignment-induced alignment effects. It should be noted that the thickness dependence observed in the measured block copolymer thermal conductivities is apparent for thicker films than those studied by Losego et al. [26]; while the reason for this difference is currently unclear, Losego et al. [26] studied a different polymeric system on bare silicon substrates, and therefore, some of the differences in thickness dependence are not surprising.

Assuming that the intrinsic thermal conductivity of the thinnest PS-b-PMMA film is similar to that of the thicker films (~ 0.19 W m⁻¹ K⁻¹, on average), the total boundary resistance of the Al/PS-b-PMMA and PS-b-PMMA/SiO₂ interfaces in the measured κ_{eff} of the thinnest samples is 24 m² K GW⁻¹, which corresponds to a thermal boundary conductance of 83 MW m⁻² K⁻¹ per interface. This value for thermal boundary conductance is in reasonable agreement with typical values across solid interfaces [48], supporting our assertion that the effective thermal conductivities measured for the thinnest films are dominated by the resistances at the sample interfaces. It is important to realize that indeed, the thermal boundary conductances across the Al/PS-b-PMMA and PS-b-PMMA/SiO₂ interfaces will most likely be different due to the fact that different materials comprise each interface; we offer this estimate of the average conductance per interface simply as a rough comparison to measurements of thermal boundary conductance in the literature.

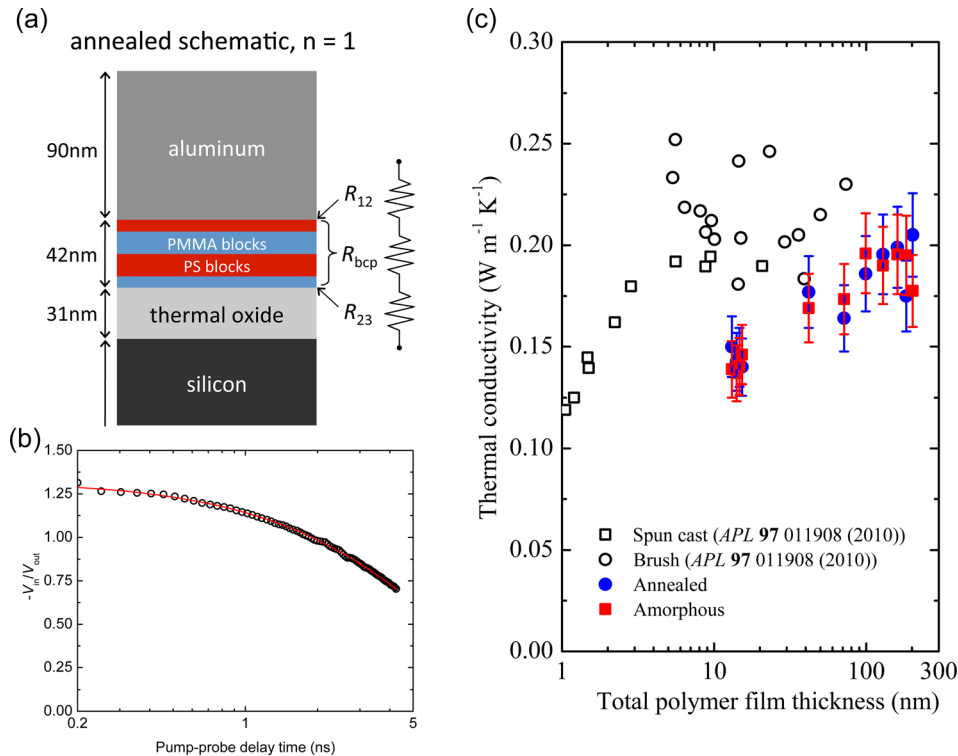


Fig. 2 (a) Schematic of TDTR film stack for assembled PS-b-PMMA sample with 1.5 lamellar period thickness, (b) example of the TDTR data and corresponding fit on the $n=0.5$ (—) annealed sample, and (c) out-of-plane thermal conductivity of annealed (filled circles) and amorphous (filled squares) PS-b-PMMA films compared to that of PMMA spun-cast films (open squares) and homopolymer brushes (open circles)

Therefore, all PS-b-PMMA films studied had approximately the same intrinsic out-of-plane κ , consistent with bulk homopolymer values. The lack of enhanced thermal transport normal to the film can be explained by the fact that only a small fraction of polymer segments (those confined near the internal block copolymer interfaces), actually undergo chain re-organization during block copolymer lamellar assembly. This results in only a small increase in the probability of longer transbonded stretches of polymer backbone lying parallel to the film normal, negligibly affecting the out-of-plane thermal conductivity in these block copolymers. These results suggest that the interfaces between the PS and PMMA, and reorganization of the PS and PMMA chains around these interfaces, do not significantly affect the thermal transport in these PS-b-PMMA films.

4 Conclusions

Lamellar phase PS-b-PMMA films with varying number of periods were formed by annealing spun-cast films of thickness commensurate with the asymmetric wetting condition, as verified by ellipsometry, XRR, and AFM. The thermal conductivity of the PS-b-PMMA films showed no enhancement in thermal conductivity upon annealing and the values were consistent with earlier studies of polymer brushes and thick spun-cast PMMA films. The results suggest that the interfaces between the PS and PMMA, and reorganization of the PS and PMMA chains around these interfaces, do not significantly affect the thermal transport in these PS-b-PMMA films. However, for thin PS-b-PMMA films, the thermal boundary resistances at the sample interfaces limit the thermal transport.

Acknowledgment

P. E. H appreciates the support from the U.S. Army Research Office (W911NF-13-1-0378). A portion of this work was supported

by the Laboratory Directed Research and Development Program at the Sandia National Laboratories. Sandia is a multiprogram laboratory operated by the Sandia Corporation, a Lockheed Martin Company, for the United States Department of Energy's National Nuclear Security Administration under Contract No. DE-AC04-94AL85000.

References

- [1] Cahill, D. G., Braun, P. V., Chen, G., Clarke, D. R., Fan, S., Goodson, K. E., Keblinski, P., King, W. P., Mahan, G. D., Majumdar, A., Maris, H. J., Phillpot, S. R., Pop, E., and Shi, L., 2014, "Nanoscale Thermal Transport. II. 2003–2012," *Appl. Phys. Rev.*, **1**(1), p. 011305.
- [2] Cahill, D. G., Ford, W. K., Goodson, K. E., Mahan, G. D., Majumdar, A., Maris, H. J., Merlin, R., and Phillpot, S. R., 2003, "Nanoscale Thermal Transport," *J. Appl. Phys.*, **93**(2), pp. 793–818.
- [3] Cahill, D. G., 2012, "Extremes of Heat Conduction—Pushing the Boundaries of the Thermal Conductivity of Materials," *MRS Bull.*, **37**(9), pp. 855–863.
- [4] Duda, J. C., Hopkins, P. E., Shen, Y., and Gupta, M. C., 2013, "Exceptionally Low Thermal Conductivities of Films of the Fullerene Derivative PCBM," *Phys. Rev. Lett.*, **110**(1), p. 015902.
- [5] Wang, X., Ho, V., Segalman, R. A., and Cahill, D. G., 2013, "Thermal Conductivity of High-Modulus Polymer Fibers," *Macromolecules*, **46**(12), pp. 4937–4943.
- [6] Shen, S., Henry, A., Tong, J., Zheng, R., and Chen, G., 2010, "Polyethylene Nanofibres With Very High Thermal Conductivities," *Nat. Nanotechnol.*, **5**(4), pp. 251–255.
- [7] Choy, C. L., Luk, W. H., and Chen, F. C., 1978, "Thermal Conductivity of Highly Oriented Polyethylene," *Polymer*, **19**(2), pp. 155–162.
- [8] Singh, V., Bougher, T. L., Weathers, A., Cai, Y., Bi, K., Pettes, M. T., McMenamin, S. A., Lv, W., Resler, D. P., Gattuso, T. R., Altman, D. H., Sandhage, K. H., Shi, L., Henry, A., and Cola, B. A., 2014, "High Thermal Conductivity of Chain-Oriented Amorphous Polythiophene," *Nat. Nanotechnol.*, **9**(5), pp. 384–390.
- [9] Guo, Z., Lee, D., Liu, Y., Sun, F., Sliwinski, A., Gao, H., Burns, P. C., Huang, L., and Luo, T., 2014, "Tuning the Thermal Conductivity of Solar Cell Polymers Through Side Chain Engineering," *Phys. Chem. Chem. Phys.*, **16**(17), pp. 7764–7771.
- [10] Duda, J. C., Hopkins, P. E., Shen, Y., and Gupta, M. C., 2013, "Thermal Transport in Organic Semiconducting Polymers," *Appl. Phys. Lett.*, **102**(25), p. 251912.

- [11] Yorifuji, D., and Ando, S., 2010, "Molecular Structure Dependence of Out-of-Plane Thermal Diffusivities in Polyimide Films: A Key Parameter for Estimating Thermal Conductivity of Polymers," *Macromolecules*, **43**(18), pp. 7583–7593.
- [12] Jin, Y., Shao, C., Kieffer, J., Falk, M. L., and Shtein, M., 2014, "Spatial Nonuniformity in Heat Transport Across Hybrid Material Interfaces," *Phys. Rev. B*, **90**(5), p. 054306.
- [13] Tynell, T., Giri, A., Gaskins, J., Hopkins, P. E., Mele, P., Miyazaki, K., and Karppinen, M., 2014, "Efficiently Suppressed Thermal Conductivity in ZnO Thin Films Via Periodic Introduction of Organic Layers," *J. Mater. Chem. A*, **2**(31), pp. 12150–12152.
- [14] Losego, M. D., Grady, M. E., Sottos, N. R., Cahill, D. G., and Braun, P. V., 2012, "Effects of Chemical Bonding on Heat Transport Across Interfaces," *Nat. Mater.*, **11**(6), pp. 502–506.
- [15] Liu, J., Yoon, B., Kuhlmann, E., Tian, M., Zhu, J., George, S. M., Lee, Y.-C., and Yang, R., 2014, "Ultralow Thermal Conductivity of Atomic/Molecular Layer-Deposited Hybrid Organic-Inorganic Zincone Thin Films," *Nano Lett.*, **13**(11), pp. 5594–5599.
- [16] Ong, W.-L., Majumdar, S., Malen, J. A., and McGaughey, A. J. H., 2014, "Coupling of Organic and Inorganic Vibrational States and Their Thermal Transport in Nanocrystal Arrays," *J. Phys. Chem. C*, **118**(14), pp. 7288–7295.
- [17] Ong, W.-L., Rupich, S. M., Talapin, D. V., McGaughey, A. J. H., and Malen, J. A., 2013, "Surface Chemistry Mediates Thermal Transport in Three-Dimensional Nanocrystal Arrays," *Nat. Mater.*, **12**(5), pp. 410–415.
- [18] Jin, Y., Shao, C., Kieffer, J., Pipe, K. P., and Shtein, M., 2012, "Origins of Thermal Boundary Conductance of Interfaces Involving Organic Semiconductors," *J. Appl. Phys.*, **112**(9), p. 093503.
- [19] Marconnet, A. M., Yamamoto, N., Panzer, M. A., Wardle, B. L., and Goodson, K. E., 2011, "Thermal Conduction in Aligned Carbon Nanotube-Polymer Nanocomposites With High Packing Density," *ACS Nano*, **5**(6), pp. 4818–4825.
- [20] Li, Q., Liu, C., and Fan, S., 2009, "Thermal Boundary Resistances of Carbon Nanotubes in Contact With Metals and Polymers," *Nano Lett.*, **9**(11), pp. 3805–3809.
- [21] Henry, A., and Chen, G., 2009, "Anomalous Heat Conduction in Polyethylene Chains: Theory and Molecular Dynamics Simulations," *Phys. Rev. B*, **79**(14), p. 144305.
- [22] Liu, J., and Yang, R., 2010, "Tuning the Thermal Conductivity of Polymers With Mechanical Strains," *Phys. Rev. B*, **81**(17), p. 174122.
- [23] Choy, C. L., Wong, Y. W., and Yang, G. W., 1999, "Elastic Modulus and Thermal Conductivity of Ultradrawn Polyethylene," *J. Polym. Sci., Part B*, **37**(23), pp. 3359–3367.
- [24] Choy, C. L., 1977, "Thermal Conductivity of Polymers," *Polymer*, **18**(10), pp. 984–1004.
- [25] Washo, B. D., and Hansen, D., 1969, "Heat Conduction in Linear Amorphous High Polymers: Orientation Anisotropy," *J. Appl. Phys.*, **40**(6), pp. 2423–2427.
- [26] Losego, M. D., Moh, L., Arpin, K. A., Cahill, D. G., and Braun, P. V., 2010, "Interfacial Thermal Conductance in Spun-Cast Polymer Films and Polymer Brushes," *Appl. Phys. Lett.*, **97**(1), p. 011908.
- [27] Kurabayashi, K., Asheghi, M., Touzelbaev, M. N., and Goodson, K., 1999, "Measurement of the Thermal Conductivity Anisotropy in Polyimide Films," *IEEE J. Microelectromech. Syst.*, **8**(2), pp. 180–191.
- [28] Griffiths, R. A., Williams, A., Oakland, C., Roberts, J., Vijayaraghavan, A., and Thomson, T., 2013, "Directed Self-Assembly of Block Copolymers for Use in Bit Patterned Media Fabrication," *J. Phys. D: Appl. Phys.*, **46**(50), p. 503001.
- [29] Jeong, S.-J., Kim, J. Y., Kim, B. H., Moon, H.-S., and Kim, S. O., 2013, "Directed Self-Assembly of Block Copolymers for Next Generation Nanolithography," *Mater. Today*, **16**(12), pp. 468–476.
- [30] PS-b-PMMA Was Obtained From Polymer Source, Inc., With 18 kDa Polystyrene and 18 kDa PMMA Blocks and Mw/Mn of 1.07. T_g for Polystyrene Block was 107 °C and T_g for PMMA Block was 133 °C.
- [31] Fredrickson, G. H., 1987, "Surface Ordering Phenomena in Block Copolymer Melts," *Macromolecules*, **20**(10), pp. 2535–2542.
- [32] Hasegawa, H., and Hashimoto, T., 1985, "Morphology of Block Polymers Near a Free Surface," *Macromolecules*, **18**(3), pp. 589–590.
- [33] Huang, E., Mansky, P., Russell, T. P., Harrison, C., Chaikin, P. M., Register, R. A., Hawker, C. J., and Mays, J., 2000, "Mixed Lamellar Films: Evolution, Commensurability Effects, and Preferential Defect Formation," *Macromolecules*, **33**(1), pp. 80–88.
- [34] Menelle, A., Russell, T. P., Anastasiadis, S. H., Satija, S. K., and Majkrzak, C. F., 1992, "Ordering of Thin Diblock Copolymer Films," *Phys. Rev. Lett.*, **68**(1), pp. 67–70.
- [35] Russell, T. P., 1996, "On the Reflectivity of Polymers: Neutrons and X-Rays," *Physica B*, **221**(1–4), pp. 267–283.
- [36] Cahill, D. G., Goodson, K. E., and Majumdar, A., 2002, "Thermometry and Thermal Transport in Micro/Nanoscale Solid-State Devices and Structures," *ASME J. Heat Transfer*, **124**(2), pp. 223–241.
- [37] Cahill, D. G., 2004, "Analysis of Heat Flow in Layered Structures for Time-Domain Thermoreflectance," *Rev. Sci. Instrum.*, **75**(12), pp. 5119–5122.
- [38] Schmidt, A. J., 2013, "Pump-Probe Thermoreflectance," *Annu. Rev. Heat Transfer*, **16**(1), pp. 159–181.
- [39] Schmidt, A. J., Chen, X., and Chen, G., 2008, "Pulse Accumulation, Radial Heat Conduction, and Anisotropic Thermal Conductivity in Pump-Probe Transient Thermoreflectance," *Rev. Sci. Instrum.*, **79**(11), p. 114902.
- [40] Hopkins, P. E., Serrano, J. R., Phinney, L. M., Kearney, S. P., Grasser, T. W., and Harris, C. T., 2010, "Criteria for Cross-Plane Dominated Thermal Transport in Multilayer Thin Film Systems During Modulated Laser Heating," *ASME J. Heat Transfer*, **132**(8), p. 081302.
- [41] Lide, D. R., 2008, *CRC Handbook for Chemistry and Physics*, Internet Version, CRC Press/Taylor and Francis, Boca Raton, FL.
- [42] Gaur, U., and Wunderlich, B., 1982, "Heat Capacity and Other Thermodynamic Properties of Linear Macromolecules. V. Polystyrene," *J. Phys. Chem. Ref. Data*, **11**(2), pp. 313–325.
- [43] Assael, M. J., Botsios, S., Gialou, K., and Metaxa, I. N., 2005, "Thermal Conductivity of Polymethyl Methacrylate (PMMA) and Borosilicate Crown Glass BK7," *Int. J. Thermophys.*, **26**(5), pp. 1595–1605.
- [44] Cahill, D. G., 1990, "Thermal Conductivity Measurement From 30 to 750 K: The 3ω Method," *Rev. Sci. Instrum.*, **61**(2), pp. 802–808.
- [45] Thomsen, C., Strait, J., Vardeny, Z., Maris, H. J., Tauc, J., and Hauser, J. J., 1984, "Coherent Phonon Generation and Detection by Picosecond Light Pulses," *Phys. Rev. Lett.*, **53**(10), pp. 989–992.
- [46] Thomsen, C., Grah, H. T., Maris, H. J., and Tauc, J., 1986, "Surface Generation and Detection of Phonons by Picosecond Light Pulses," *Phys. Rev. B*, **34**(6), pp. 4129–4138.
- [47] Lee, H., 1982, "Rapid Measurement of the Thermal Conductivity of Polymer Films," *Rev. Sci. Instrum.*, **53**(6), pp. 884–887.
- [48] Hopkins, P. E., 2013, "Thermal Transport Across Solid Interfaces With Nanoscale Imperfections: Effects of Roughness, Disorder, Dislocations, and Bonding on Thermal Boundary Conductance," *ISRN Mech. Eng.*, **2013**, p. 682586.